CLOUD PARAMETERS FROM GOES VISIBLE AND INFRARED RADIANCES DURING THE FIRE CIRRUS IFO, OCTOBER 1986

Patrick W. Heck and David F. Young
Aerospace Technologies Division, Planning Research Corporation
Hampton, Virginia 23666
and
Patrick Minnis and Edwin F. Harrison
Atmospheric Sciences Division, NASA Langley Research Center
Hampton, Virginia 23665-5225

1. Introduction

Visible (VIS, 0.65 μm) and infrared (IR, 10.5 μm) channels on geostationary satellites are the key elements of the International Satellite Cloud Climatology Project (ISCCP). All daytime ISCCP cloud parameters are derived from a combination of VIS and IR data. Validation and improvement of the ISCCP and other cloud retrieval algorithms are important components of the First ISCCP Regional Experiment (FIRE) Intensive Field Observations (IFO). Data from the Cirrus IFO (October 19 - November 2, 1986) over Wisconsin are available for validating cirrus cloud retrievals from satellites. The Geostationary Operational Environmental Satellite (GOES) located over the Equator at approximately 100°W provided nearly continuous measurements of VIS and IR radiances over the IFO area. This paper presents the preliminary results of cloud parameters derived from the IFO GOES data. Cloud altitudes are first derived using an algorithm without corrections for cloud emissivity. These same parameters will then be computed from the same data relying on an emissivity correction algorithm based on correlative data taken during the Cirrus IFO.

2. Data and methodology

A cloud parameter retrieval scheme, the hybrid bispectral threshold method (HBTM) described by Minnis et al. (1987), was applied to the GOES 1-km VIS and 4-km IR radiances taken between 47°N and 42°N and between 87°W and 92°W. This 5° box was divided into a 0.5° grid for analysis. Clear-sky temperature and albedo as well as cloud amount, temperature (height), and cloud albedo were derived over each of the 100 regions at each daylight half hour during the experiment. These cloud properties were also derived for a low-level layer (< 2 km altitude), a middle layer (between 2 km and 6 km), and a high layer (> 6 km). For these preliminary results, a lapse rate of 6.5 °K/km was assumed in order to infer the cloud altitude from the derived cloud temperature.

Both narrowband VIS and broadband shortwave (SW) albedos were derived from the VIS data. The GOES VIS counts (D) were converted to narrowband radiance with the calibration of Whitlock (1987) and then converted to albedo by dividing by the incoming solar radiance at 0.65 μm, the cosine of the solar zenith angle (SZA), and a bidirectional reflectance anisotropic factor (Minnis and Harrison, 1984). Shortwave albedo was determined in a similar fashion except that the incoming radiance covered the entire solar spectrum and the VIS counts were converted to broadband (0.2 μm - 5.0 μm) radiance. Narrowband-broadband conversions were performed in a manner similar to that described by Harrison et al. (1988) except that GOES and NOAA-9 ERBE (Earth Radiation Budget Experiment) data were used. Since these satellites operate in different orbits, only selected data from matching fields of view over the entire GOES field-of-view were used to effect the

correlation. The dissimilar scan patterns of the two satellites' instruments dictated more liberal matching constraints than those used by Minnis and Harrison (1984). Broadband longwave (5.0 - 50.0 μm) data were fit to the correlated IR data with a quadratic yielding an RMS difference of 4% over water and 6% over land. With the availability of the varying SZA from the GOES it was determined that a model of the form

$$L_{sw} = a_1 D + a_2 D^2 + a_3 D \ln(\sec(SZA))$$

best described the shortwave radiances, producing RMS differences of 13% over water and 18% over land. This result and the data are shown in Fig. 1.

A critical factor for the HBTM and other algorithms is the accurate specification of clear-sky conditions. With the long time series of GOES data, it was possible to determine the half-hourly clear-sky albedo for the IFO by measuring the minimum VIS counts on days which were predominantly clear. This process was performed utilizing data primarily from Oct. 19 resulting in a 0.1^0 map of both VIS and SW clear-sky albedo. Clear-sky temperature was derived in the manner given by Minnis et al. (1987).

3. Results

Examples of the clear-sky albedo maps averaged to the IFO grid is given in Fig. 2 for 1800 UT. Values of VIS albedo over the IFO "diamond" (asterisks in the figures) range from 10 - 12%, while the SW albedos vary from 15 - 17%. In the afternoon (not shown), the VIS albedos are much lower than the broadband values which are as high as 29%. The usual trends in daily variation of this parameter are seen in Fig. 3 for the region containing Wausau (top asterisk in Fig.2). A time series of daytime (1500 - 2200 UT) cloud amounts and clear-sky and cloud temperatures are given in Figs. 4 and 5, respectively, for the region containing Ft. McCoy (left asterisk in Fig. 2). The high variability is due to the small size of the region. These plots show that it was clear over the region on Oct. 19 and 21 and overcast on Oct. 22, 31, and from Oct. 24 through 26. Variable cloudiness occurred on the remaining days. These cloud amounts are consistent with surface observations as reported by Hahn et al. (1988). Clear-sky temperatures show a significant diurnal cycle on days with clear or partly cloudy skies. On overcast days, an interpolation scheme was used to obtain clear-sky temperatures. Cloud temperatures suggest low clouds on Oct. 20, 23, 26, 29, and 30 and midlevel clouds on Oct. 22, 25, and 31. The only days with obviously high clouds are Oct. 22, 25, and 31. The nominal HBTM assumes that the clouds can be treated as black bodies so that the mean observed temperature over areas determined to be cloudy is the cloud-top temperature. It is known that many cirrus clouds are non-black and, therefore, the HBTM will probably underestimate their altitudes. Surface and aircraft observations (FIRE, 1987) indicate that high clouds were present over the area on days Oct. 22, 25, and 31 together with lower clouds. High clouds without underlying decks were also reported on days Oct. 27, 28, and 30. Only cirrus was reported on the latter 3 days. Thus, it is apparent that some correction for cirrus emissivity is necessary to correctly identify the true cloud altitudes.

Figure 6 shows the cloud cover derived from GOES data taken at 1500 UT, Oct. 28. Mostly cloudy areas are found in the northern part of the grid. The thickest parts of the cirrus are found in the northern corners and central part of the grid as inferred from the cloud temperatures in Fig. 7. By 2030 UT (Fig. 8), the cloud pattern still shows the most widespread

cloudiness over the north with some mostly cloudy areas around Ft. McCoy. Significant high cloudiness was detected west of Green Bay and near Ft. McCoy with the remainder being classified primarily as midlevel clouds. The cloud patterns derived from the AVHRR data (Fig. 9) with the same algorithm (see Harrison et al., 1988) about one-half hour later are very similar but shifted to the east.

4. Concluding remarks

A preliminary set of cloud parameters derived from GOES data provide a continuous quantification of clouds over the Cirrus IFO. Initial comparisons with the IFO data show that total cloud amount is generally consistent with surface reports. Cloud altitude, however, appears to be substantially underestimated for cirrus. By making use of emissivity computations (Minnis et al., 1988) derived from IFO intercomparisons, it will be possible to greatly improve the techniques for determining cirrus cloud heights.

5. References

FIRE Science Experiment Team Workshop, 1987. Linithicum, MD, Nov. 9-12.

Hahn, C. J., S. G. Warren, and J. L. London, 1988: Surface Synoptic Cloud Reports. FIRE Internal Report, February.

Harrison, E. F., P. Minnis, B. A. Wielicki, P. W. Heck, S. K. Gupta, D. F. Young, and G. G. Gibson, 1988: ERBE and AVHRR Cirrus Cloud FIRE Study. FIRE Workshop, Vail, CO, July 11-15.

Minnis, P. and E. F. Harrison, 1984: Diurnal Variability of Regional Cloud and Clear-Sky Radiative Parameters Derived From GOES. J. Clim. Appl. Meteor., 23, 993-1051.

Minnis, P., E. F. Harrison, and G. G. Gibson, 1987: Cloud Cover Over the Equatorial Eastern Pacific Derived From July 1983 ISCCP Data Using a Hybrid Bispectral Threshold Method. J. Geophys. Res., 92, 4051-4073.

Minnis, P., J. M. Alvarez, D. F. Young, P. W. Heck, and K. Sassen, 1988: Cirrus Cloud Properties Derived From Coincident GOES and Lidar Data During the 1986 FIRE Cirrus Intensive Field Observations. FIRE Workshop, July 11-15.

Whitlock, C. H., 1987: Satellite Calibration Values for the FIRE/SRB Wisconsin Experiment, NASA memo, December 8.

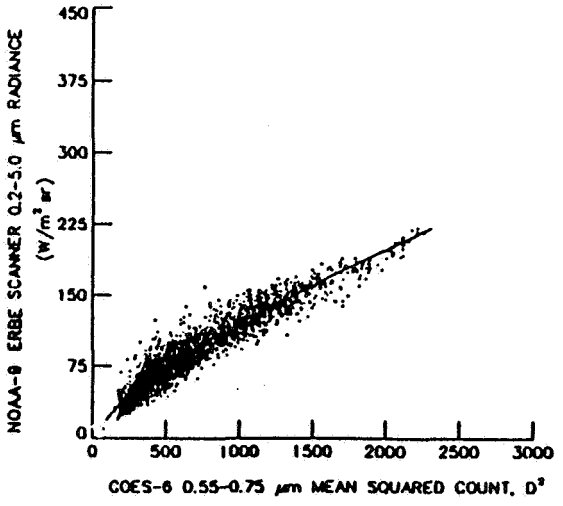

Figure 1. Correlation of ERBE broadband and GOES narrowband shortwave radiances for October, 1986. Curve is for solar zenith of 55°.

(a) Narrowband albedo

(b) Broadband albedo

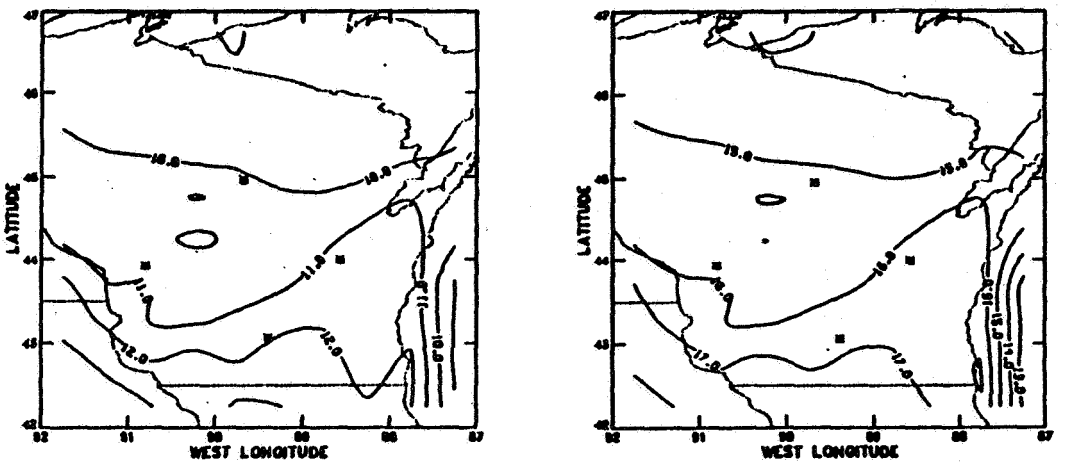

Figure 2. Clear-sky albedo(%) for 1800 UT, October 28, 1986.

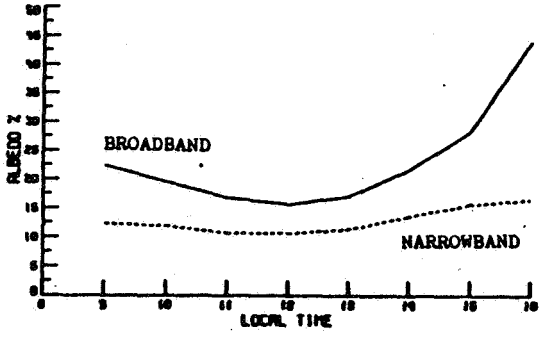

Figure 3. Daytime clear-sky albedo(%) over Wausau for October 28, 1986.

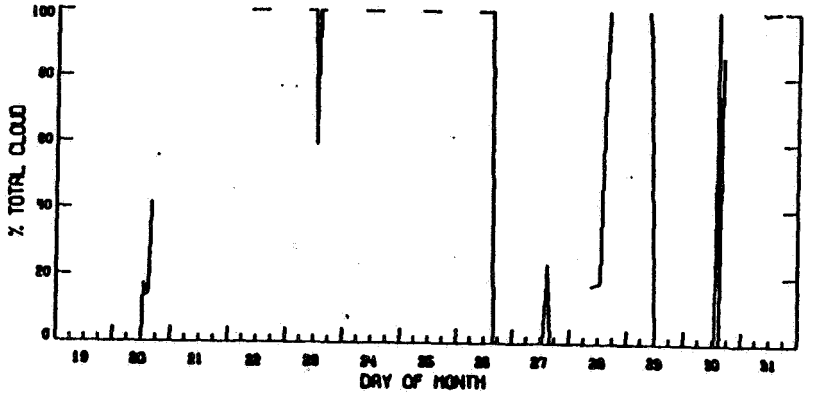

Figure 4. Time series of cloud cover(%) over Ft. McCoy, Oct. 19-31, 1986.

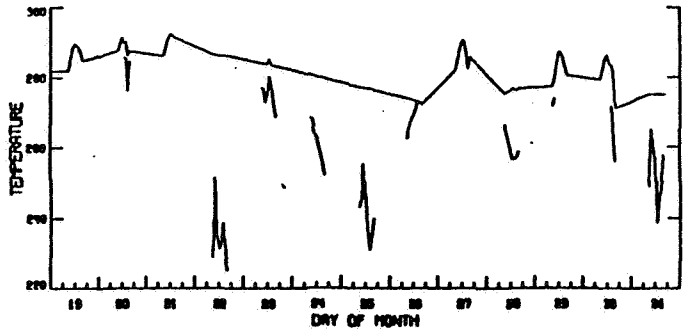

Figure 5. Time series of clear-sky temperature(K, continuous line) and cloud temperature(K) over Ft. McCoy, October 19-31, 1986.

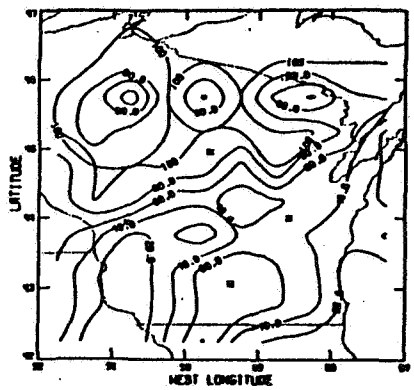

Figure 6. Total cloud cover(%) for 1500 UT, Oct. 28, 1986.

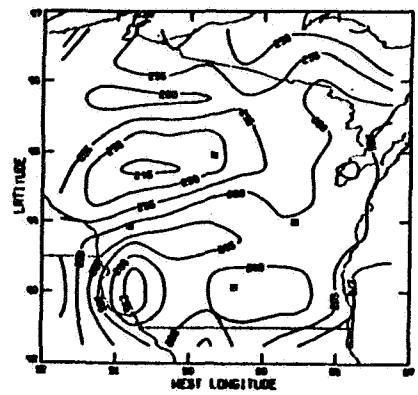

Figure 7. Cloud temperature(K) for 1500 UT, Oct. 28, 1986.

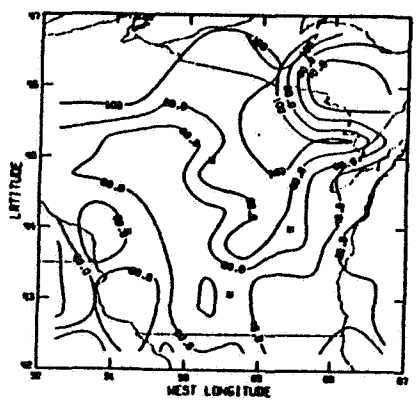

Figure 8. Total cloud cover(%) for 2030 UT, Oct. 28, 1986.

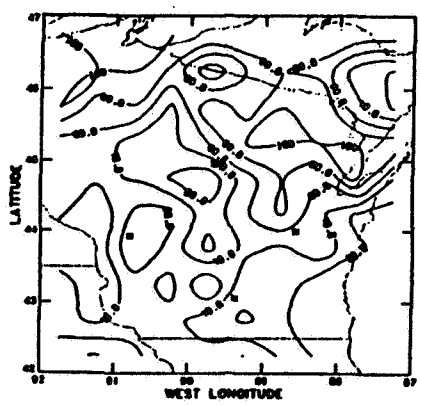

Figure 9. Total cloud cover(%) derived from AVHRR for 2100 UT, Oct. 28, 1986.